Materials Chemistry and Physics 136 (2012) 796–801

Contents lists available at SciVerse ScienceDirect

Materials Chemistry and Physics

journal homepage: www.elsevier.com/locate/matchemphys

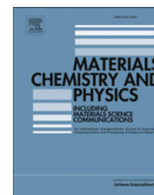

Influence of Mg-containing precursor flow rate on the structural, electrical and mechanical properties of Mg-doped GaN thin films

Wen-Cheng Ke [a], Sheng-Rui Jian [b,*], I-Chen Chen [c], Jason S.-C. Jang [c], Wei-Kuo Chen [d], Jenh-Yih Juang [d]

[a] Department of Mechanical Engineering, Yuan Ze University, Chung-Li 320, Taiwan
[b] Department of Materials Science and Engineering, I-Shou University, Kaohsiung 840, Taiwan
[c] Institute of Materials Science and Engineering, National Central University, Chung-Li 320, Taiwan
[d] Department of Electrophysics, National Chiao Tung University, Hsinchu 300, Taiwan

HIGHLIGHTS

- ► The GaN:Mg thin films are grown by MOCVD.
- ► Electrical properties of GaN:Mg thin films are measured by Hall measurement.
- ► Hardness and Young's modulus of GaN:Mg thin films are measured by nanoindentation.

GRAPHICAL ABSTRACT

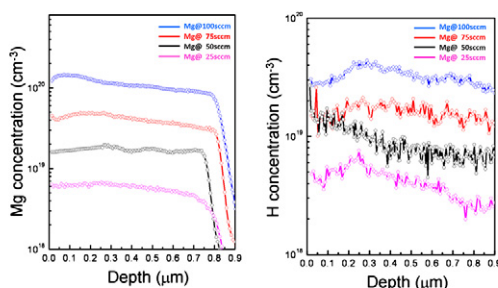

ARTICLE INFO

Article history:
Received 1 January 2012
Received in revised form
19 July 2012
Accepted 31 July 2012

Keywords:
Thin films
CVD
Hall effect
Nanoindentation

ABSTRACT

The effects of Mg-containing precursor flow rate on the characteristics of the Mg-doped GaN (GaN:Mg) were systematically studied in this study. The GaN:Mg films were deposited on sapphire substrates by metal-organic chemical-vapor deposition (MOCVD) with various flow rates of 25, 50, 75 and 100 sccm of bis-(cyclopentadienyl)-magnesium (Cp2Mg) precursor. The structural, electrical and nanomechanical properties of GaN:Mg thin films were characterized by X-ray diffraction (XRD), atomic force microscopy (AFM), Hall measurement and nanoindentation techniques, respectively. Results indicated that GaN:Mg films obtained with 25 sccm Cp2Mg possess the highest hole concentration of 3.1×10^{17} cm^{-3}. Moreover, the hardness and Young's modulus of GaN:Mg films measured by a Berkovich nanoindenter operated with the continuous contact stiffness measurements (CSM) option showed positive dependence with increasing flow rate of Cp2Mg precursor, presumably due to the solution hardening effect of Mg-doping.
© 2012 Elsevier B.V. All rights reserved.

1. Introduction

Successful preparation of *p*-type GaN:Mg layer has been one of the vital challenges for realizing blue and green light emitting diodes (LEDs). The primary function of this layer is to supply enough concentration of holes so that, when injected into the active layer, they will recombine with electrons and emit light efficiently. Therefore, a higher hole concentration in the *p*-GaN layer is beneficial to the increase of the light intensity of LEDs. In addition, the dopant concentration in the *p*-GaN layer also must be optimized to obtain ohmic metal contact, which is essential to reduce the operating voltage of the devices. However, since Mg dopants are deep acceptors with relative large ionization energy (~160 meV from the valence band), the maximum hole carrier concentration of *p*-GaN thin films obtained by Mg doping has been severely limited [1]. To date, several growth techniques, such as delta-doping [2], Mg–O [3] or Mg–Zn co-

* Corresponding author. Tel.: +886 7 6577711x3130; fax: +886 7 6578444.
E-mail address: srjian@gmail.com (S.-R. Jian).

0254-0584/$ – see front matter © 2012 Elsevier B.V. All rights reserved.
http://dx.doi.org/10.1016/j.matchemphys.2012.07.060

doping [4], and multilayered buffer [5], have been demonstrated with some successes in increasing the hole concentration of *p*-GaN thin films. High hole carrier concentrations (i.e. $> 1 \times 10^{18}$ cm^{-3}) with very low resistivities in the modulation Mg-doped *p*-type $Al_xGa_{1-x}N$/GaN superlattices has been reported and was attributed to the significant reduction in activation energy [6]. However, the hole concentration of the doped *p*-type $Al_xGa_{1-x}N$/GaN superlattices mainly depends upon the Al content in the $Al_xGa_{1-x}N$ layer. In order to achieve a high Al content in the AlGaN thin films, the growth pressure must be reduced as much as possible such that the serious parasitic reaction of precursors TMAl and NH_3 in the MOCVD reactor can be minimized [7,8]. The typical growth pressure of *p*-type $Al_xGa_{1-x}N$/GaN doped superlattices has been kept at around ~50 mbar. It implies that, in order to grow single layer of either *p*-AlGaN or *p*-GaN films with high doping concentration, it is essential to reduce the growth pressure. Unfortunately, up to now, most of the previous reports of growing *p*-GaN thin films have been focused on high growth pressure practiced in the commercial MOCVD systems [1–5].

In addition to monitoring the electric properties through careful control of the processing parameters, successful fabrication of devices based on Mg-doped GaN thin films also requires better understanding of the mechanical characteristics of the films, since the contact loading during processing or packaging can significantly degrade the performance of these devices. The mechanical properties of materials are size-dependent. Thin films may have very different mechanical properties from their bulk materials. Consequently, a precise measurement of the mechanical properties of GaN:Mg thin films is required to use them as structural/functional elements in the devices. Nanoindentation is a versatile and non-destructive technique for measuring the mechanical characteristics of small structures [9,10] or thin films and coatings [11–15] at very small scales, namely in the micron and sub-micron range. The load-displacement responses obtained during nanoindentation also provide substantial insights into the mode and onset of plastic deformations or fracture of the materials [16].

In the present study, we attempted to grow *p*-GaN films under the very low pressure of 50 mbar. The experimental results show that the decrease in growth pressure effectively increases the Mg doping efficiency for the *p*-GaN films. The *p*-GaN thin films obtained under the low pressure MOCVD processes all display excellent structural quality with very smooth surface, as revealed by X-ray diffraction (XRD) and atomic force microscopy (AFM). The electrical and nanomechanical characteristics of the present MOCVD-derived *p*-type GaN:Mg thin films were characterized by Hall measurements and by using a Berkovich nanoindentation system operated in the continuous contact stiffness measurement (CSM) mode, respectively. Effects of the Mg-doping concentration on the electrical and mechanical properties of the obtained GaN:Mg thin films are discussed.

2. Experimental details

The *p*-GaN thin films were grown in a horizontal MOCVD system using trimethylgallium (TMGa), ammonia (NH_3) and bis (cyclopentadienyl) magnesium (Cp2Mg) as the metal-organic precursors for Ga, N and Mg, respectively. A series of ~0.8-μm-thick Mg-doped GaN films with different acceptor concentrations were grown on templates consisting of a layer of 0.2-μm-thick undoped-GaN and a layer of LT-GaN both coated sequentially on the sapphire substrates, hereafter denoted as (un-GaN)/LT-GaN buffer/sapphire. The growth temperature of the *p*-GaN thin films was set at 1100 °C. The concentration of Mg doping was controlled by varying the flow rate of Cp2Mg from 25 sccm to 100 sccm. Afterwards, annealing was carried out in a nitrogen environment at a temperature of 700 °C for 30 min to depassivate the Mg–H complexes, which turns out is a very crucial step of achieving high hole concentration in the resultant *p*-GaN thin films. The Mg concentration and surface morphology of *p*-GaN films were measured by a secondary ion mass spectrometer (SIMS) and AFM, respectively. The crystalline structures of the GaN:Mg thin films were mainly characterized by the high resolution X-ray diffraction (HRXRD, BRUKER D8 DISCOVER) ω-scan rocking curve. The hole concentration of the *p*-GaN thin films was measured using the Hall system with high purity indium balls pressed onto the four corners as electrical contacts following the van der Pauw geometry configuration.

The mechanical properties of the GaN:Mg thin films were characterized using an MTS NanoXP® system (MTS Cooperation, Nano Instruments Innovation Center, TN, USA). The nanoindentation measurements, using a three-side pyramidal Berkovich diamond indenter of 50 nm radius (faces 65.3° from vertical axis), were conducted under the continuous stiffness measurement (CSM) procedures [17], which was accomplished by superimposing small oscillations on the primary loading signal and analyzing the resultant responses of the system by using a lock-in amplifier. Prior to real measurement, the indenter was loaded and unloaded three times to ensure that the tip was properly in contact with the surface of GaN:Mg thin films and that any parasitical phenomenon was completely excluded from the measurement. On the fourth time, the indenter was loaded at a strain rate of 0.05 s^{-1} until reaching an indent depth (h_c) of 80 nm and was held for 30 s. Then, it was withdrawn with the same strain rate until 10% of the peak load was reached. At least 20 indents were performed on each sample. Each indentation was separated by 50 μm to avoid possible interferences between neighboring indents. We also followed the analytic method proposed by Oliver and Pharr [18] to determine the hardness and Young's modulus of GaN:Mg thin films from the load-displacement results. In this way, hardness and Young's modulus were obtained as a continuous function of penetration depth.

3. Results and discussion

The results of hole concentration for all the GaN:Mg films obtained by the room-temperature Hall measurements are listed in Table 1. It is evident from Table 1 that the film with the highest hole concentration of 3.1×10^{17} cm^{-3} is the one obtained with a Cp2Mg flow rate of 25 sccm and it starts to decrease monotonically to 4.7×10^{16} cm^{-3} for film obtained with 100 sccm Cp2Mg flow rate, albeit the SIMS analyses (as shown in Fig. 3(a)) have otherwise

Table 1
Properties of GaN:Mg thin films grown at various Mg flow rates.

Mg-doped GaN films[a] Mg flow rate	R_σ (nm)	H (GPa)	E_{film} (GPa)	τ_{max} (GPa)	Screw/edge dislocation density (cm^{-2})	Hole concentration (cm^{-3})
25 sccm	0.72	20.5 ± 0.9	308.2 ± 2.6	6.8 ± 0.3	$1.56 \times 10^8/9.64 \times 10^8$	3.1×10^{17}
50 sccm	2.29	22.5 ± 0.6	335.6 ± 4.9	7.5 ± 0.2	$2.19 \times 10^8/1.19 \times 10^9$	1.3×10^{17}
75 sccm	5.28	25.1 ± 0.8	376.1 ± 3.7	8.4 ± 0.3	$2.44 \times 10^8/1.22 \times 10^9$	5.5×10^{16}
100 sccm	23.45	28.5 ± 1.6	409.8 ± 6.6	9.5 ± 0.5	$2.83 \times 10^8/1.35 \times 10^9$	4.7×10^{16}
		19 ± 1 [25]	286 ± 25 [25]	6.3 [25]		$1.7 - 6.0 \times 10^{17}$ [19]

[a] This study.

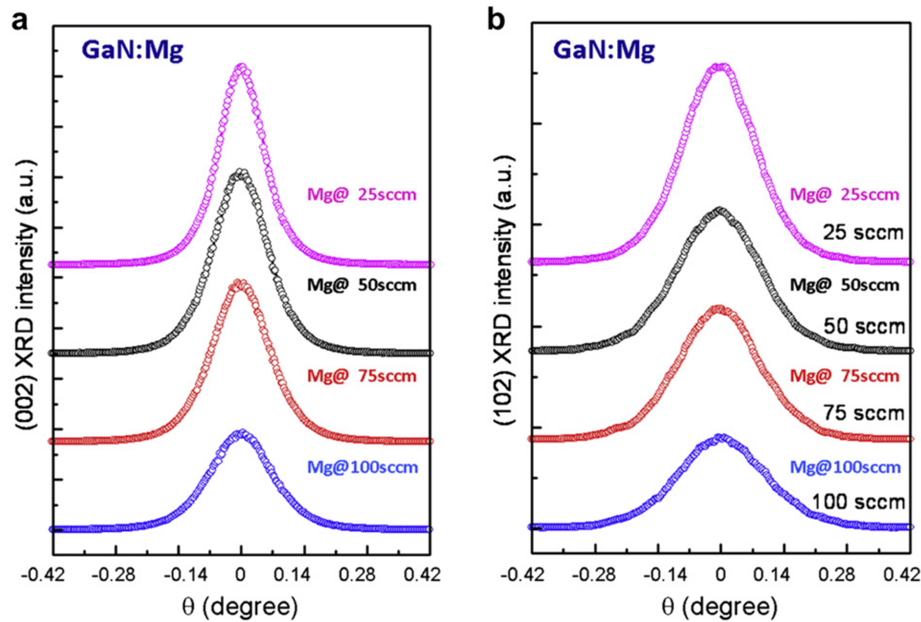

Fig. 1. The ω-scans (rocking curve) from (a) (002) and (b) (102) XRD measurement for various Mg flow rates of GaN:Mg thin films.

indicated that the Mg concentration increases from 0.07% to 0.27% for the 25 sccm and 100 sccm films, respectively. The apparent discrepancy may be attributed to the effect originated from hydrogen involved in the GaN growth processes. Hydrogen behaves as a donor and forms neutral (Mg–H) complexes with acceptors, which further suppresses the formation of self-compensating native point defects (e.g. nitrogen vacancy, V_N) [19,20]. As a result, the high concentration of hydrogen incorporated during the film growth processes became the main factor limiting the hole concentration in the obtained GaN:Mg thin films. It has been suggested that the Mg–H complexes can be depassivated to render the acceptor electrically active by thermal annealing in nitrogen environment.

Alternatively, the quality of the crystalline structure of GaN:Mg films can play a key role in influencing the eventual hole concentrations. Wright et al. [21] proposed that the edge dislocations may behave as hole traps in *p*-type GaN thin films. In order to delineate the effects of Mg-doping on the film crystalline structure and hence on the resulting hole concentration, high resolution XRD measurements, especially the XRD spectra of (002) and (102) diffraction peaks were carried out. Fig. 1(a) shows the full width at half maximum (FWHM) values of the (002) peak. It indicates that the FWHM value decreases from 0.14° to 0.11° as the flow rate of Cp2Mg precursor decreases from 100 sccm to 25 sccm. Similarly, as shown in Fig. 1(b), the FWHM of the (102) diffraction peak also decreases from 0.20° to 0.17° with decreasing Cp2Mg flow rate. These results suggest that an increasing Cp2Mg flow rate may have resulted in increased density of screw and edge dislocations in the doped *p*-GaN thin films. Based on the premise that the [002] and [102] diffraction peaks are respectively affected by screw and edge dislocations, the respective dislocation density (ρ) can be calculated by using the following expression [22]:

$$\rho = \frac{\beta^2}{4.35\, b^2} \quad (1)$$

where *b* is the absolute value of the Burgers vector and β is the FWHM of the corresponding diffraction peak. The obtained densities of the screw and edge dislocations in the GaN:Mg thin films are listed in Table 1. Since the atomic radius of Mg (~0.136 nm) is larger than that of Ga atom (~0.126 nm), an increasing strain field induced by Mg doping can be expected. Typically, in a strained thin film, any further deposition would result in formation of dislocations such that the accumulated strain can be accommodated and the morphology of the layer remains smooth. In this scenario, the reduced hole concentration with increasing Mg doping may be explained by the resultant dislocation densities.

Fig. 2 displays the surface morphologies of the 25 sccm (left panel) and 100 sccm (right panel) GaN:Mg films. It is evident that the surface roughness (*R*a) within a scanning area of 10 × 10 μm^2 shows a dramatic change from 0.72 to 23.45 nm (as listed in Table 1), when the Mg doping is increased and the surface morphology drastically changes from rather smooth continuous film to densely distributed hexagonal hillocks seen in Fig. 2. We note that, in fact, such morphology changes were actually appearing when the Cp2Mg flow rate was increased to 75 sccm (not shown here). It has been reported that Mg doping can result in pyramidal-shaped extensive defects in the resultant GaN films when the Mg concentration exceeds 10^{20} cm^{-3} [23]. This is quite consistent with the Mg concentrations of the present GaN:Mg films obtained by SIMS. Fig. 3(a) shows the SIMS depth profile analyses revealing the actual Mg atomic concentration in GaN:Mg thin films grown by the present low pressure growth technique. The procedure of converting the sputtering into the SIMS depth profile is briefly described as following. Firstly, a testing experiment for calculating the sputtering rate was performed for each sample before doing the element concentration depth profile analysis. The testing experiment comprises: (i) measuring the depth of craters created on the polished surface of GaN:Mg samples by surface profiler after a certain sputtering time; and (ii) dividing the measured depths by the sputtering time to obtain the sputtering rate. Since in each case the sputtering rate was obtained under exactly identical oxygen or cesium ion bombardment conditions, it could be correctly converted to the SIMS depth profiles of the corresponding GaN:Mg samples. It is evident that the Mg concentration remains rather uniform throughout the entire thickness of GaN:Mg thin film and at a depth of 0.4 μm the Mg concentrations were 1.07×10^{20}, 4.09×10^{19}, 1.62×10^{19} and 6.22×10^{18} atom/cm^3,

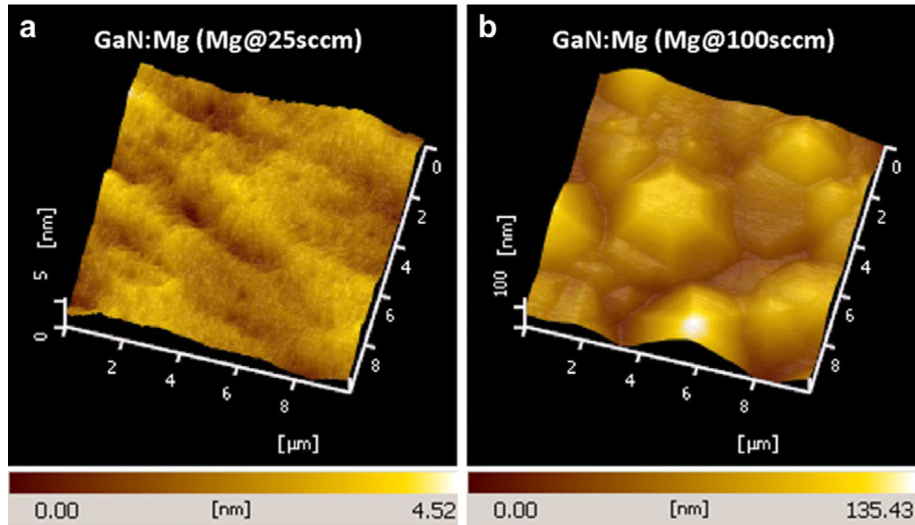

Fig. 2. AFM image of GaN:Mg thin films with various Mg flow rates of (a) 25 sccm and (b) 100 sccm.

for the Mg flow rate of 100, 75, 50 and 25 sccm, respectively. The SIMS analysis of H concentration in GaN:Mg thin films is also displayed in Fig. 3(b). It can be observed that the H concentration is slightly increased with increasing Mg flow rate. It is, thus, quite reasonable to attribute the increase in hole concentration to the decrease of H concentration in GaN:Mg thin films [24].

It should be noted that the sample with the highest Mg concentration appears to be over-doped with an estimated Mg/Ga ratio of 0.49%, which is responsible for the severely degraded surface morphology consisting of densely packed hexagonal hillocks seen in the right panel of Fig. 2. In addition, the over-doped GaN:Mg could also lead to significant reduction in hole concentration, since Mg may incorporate into electrically inactive complexes and/or generate compensating donors. Consequently, it is suggestive from the present results that, for simultaneously achieving high hole concentration and smooth surface morphology, the optimal Mg doping concentration should be kept around 6.22×10^{18} atom/cm^3 in GaN:Mg thin films obtained by the low pressure CVD process practiced in the present study.

Typical results of nanoindentation measurements for the GaN:Mg films investigated in the present study are displayed in Fig. 4. The load-displacement curve for GaN:Mg thin films with the highest Mg doping is shown in Fig. 4(a). The load-displacement response obtained by nanoindentation contains information about the elastic and plastic deformation of the indented materials. Thus, it is often regarded as the “fingerprint” of the films under investigation, because mechanical properties, such as the hardness and Young’s modulus, can be readily extracted from the load-displacement data [18]. The hardness is estimated by the expression:

$$H = P_{\max}/A_c \tag{2}$$

where $P_{\max}$ is the peak load; A_c is the contact projected area determined by the geometry of the indenter and the contact depth, h_c. In the present work, A_c is assumed to be describable by an area function $F(h_c)$ and can be expressed as,

$$A_c = F(h_c) = 24.69h_c^2 + 122.80h_c^1 + 212.77h_c^{1/2} - 191.25h_c^{1/4} - 32.77h_c^{1/8} \tag{3}$$

The elastic modulus is then determined from the following relation:

$$E_{eff} = \frac{1}{2\beta} S \sqrt{\frac{\pi}{A_c}} \tag{4}$$

with S and β being respectively denoted as the measured stiffness and a shape constant of 1.034 for a Berkovich indenter. The E_{eff} is the effective elastic modulus defined by

$$\frac{1}{E_{eff}} = \frac{1-\nu_{film}^2}{E_{film}} + \frac{1-\nu_i^2}{E_i} \tag{5}$$

which takes into account the fact that elastic displacements occur in both the thin film and an indenter. The elastic modulus E_i, and Poisson’s ratio, ν_i, of the Berkovich indenter used in this work are 1141 GPa and 0.07, respectively [18]. The Poisson’s ratio of thin film (ν_{film}) is assumed to be 0.25 [25]. By combining Eqs. (4) and (5), one obtains the Young’s modulus of GaN:Mg thin films, E_{film}, as following:

$$E_{film} = \frac{\left(1-\nu_{film}^2\right) S E_i \sqrt{\pi}}{2\beta E_i \sqrt{A_c} - \left(1-\nu_i^2\right) S \sqrt{\pi}} \tag{6}$$

Through the continuous contact stiffness measurements, the displacement dependence of hardness and Young’s modulus are obtained instantaneously. Fig. 4(b) displays the hardness versus penetration depth curves for GaN:Mg thin films deposited at the various Cp2Mg flow rates. All of the plots can be divided into two stages, namely, initial increase to a maximum value and subsequent precipitous drop to a relatively constant value. The increase in hardness at the early stage of penetration is usually attributed to the transition between purely elastic to elastic/plastic contact. As a result, the hardness cannot be accurately measured by the mean contact pressure at this stage. Only under the condition of a fully developed plastic zone does the mean contact pressure represent the hardness. When there is no plastic zone, or only partially formed plastic zone, the mean contact pressure is less than the nominal hardness [18]. On the other hand, the constant characteristic of hardness reached after the first stage is consistent with that of a single material; therefore, the hardness values obtained at this stage could be regarded as the intrinsic properties of the films. The obtained hardness for GaN:Mg thin films grown under Cp2Mg

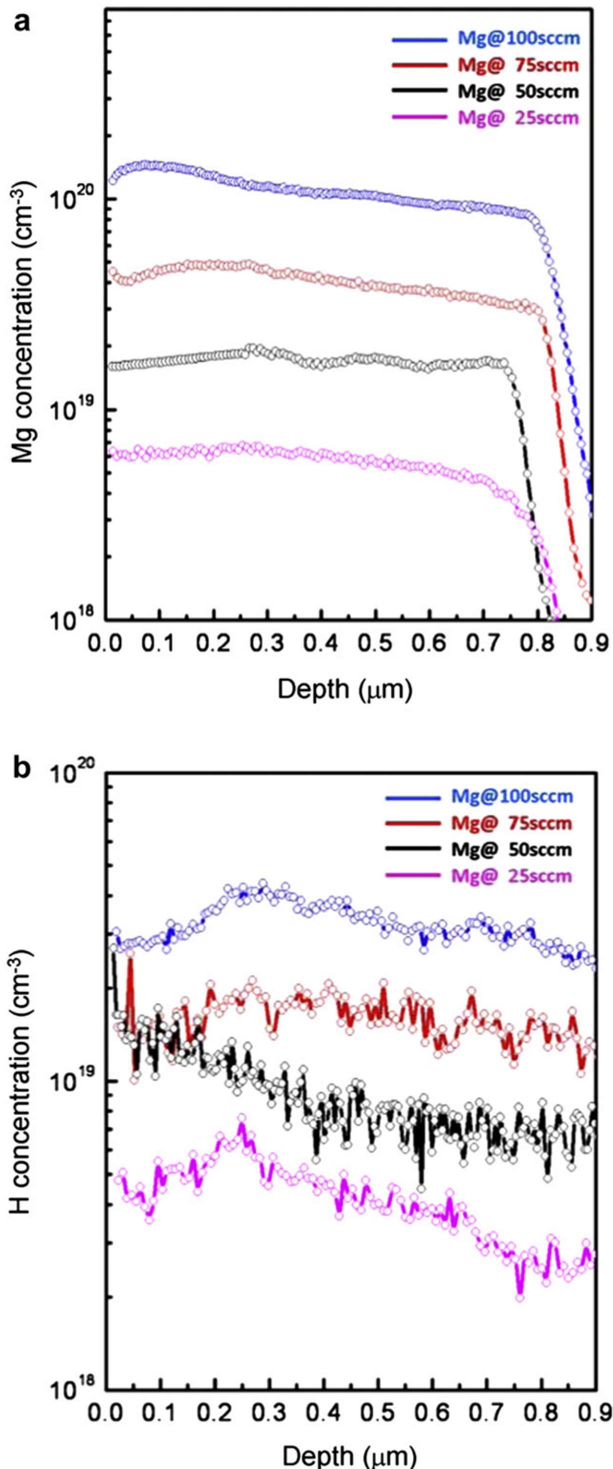

Fig. 3. SIMS analysis for GaN:Mg thin films with various Mg flow rates: (a) Mg and (b) H concentration profiles.

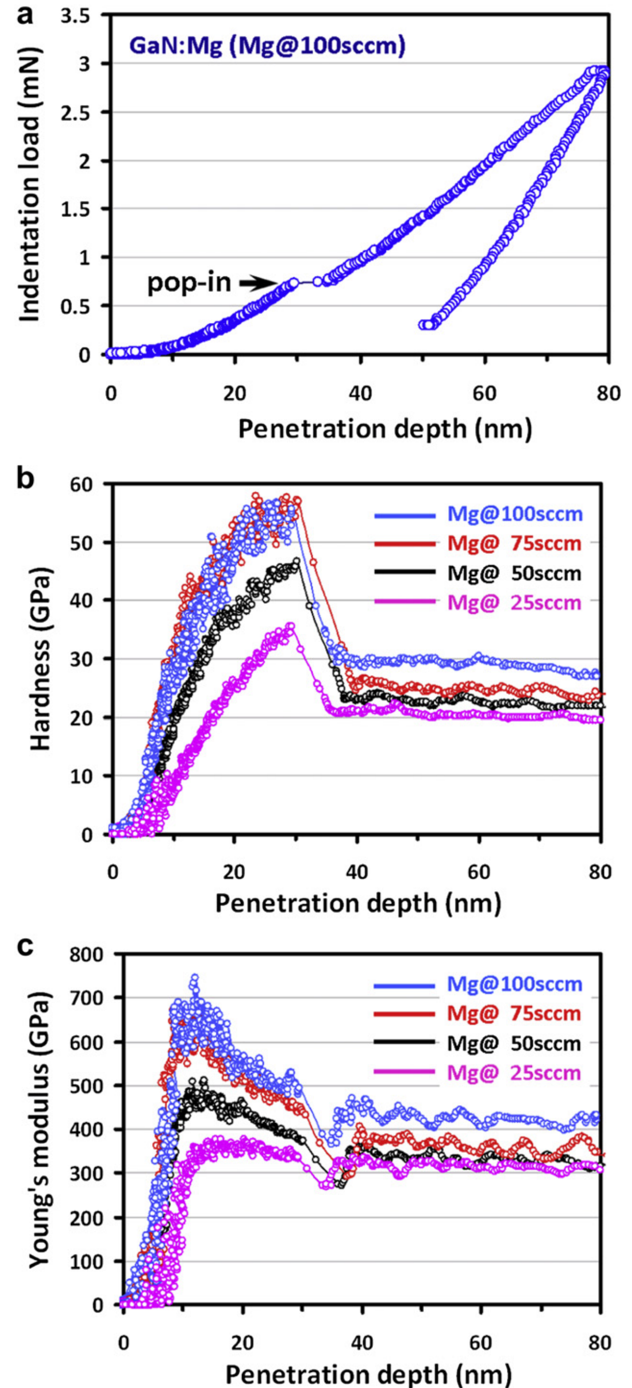

Fig. 4. Nanoindentation results: (a) the typical load-displacement curve for GaN:Mg thin films deposited at the Mg flow rate of 100 sccm; (b) hardness–displacement curves and (c) Young's modulus–displacement curves for GaN:Mg thin films.

flow rate of 25, 50, 75 and 100 sccm are 20.5 ± 0.9, 22.5 ± 0.6, 25.1 ± 0.8 and 28.5 ± 1.6 GPa, respectively. A clear trend can be observed from this figure that the hardness increases with increasing Mg doping concentration. Similar tendency is also clearly observed for the Young's modulus of GaN:Mg thin films as displayed in Fig. 4(c). The corresponding values of the Young's modulus for are 308.2 ± 2.6, 335.6 ± 4.9, 376.1 ± 3.7 and 409.8 ± 6.6 GPa, respectively.

Back to the load-displacement curve displayed in Fig. 4(a). It can be clearly observed that the loading segment of the curve consists of a series of serrations all the way up the maximum load with a single prominent pop-in event (indicated by the arrow) occurring at a relatively low critical pop-in indentation load P_{cr}. The pop-in event is a signature of catastrophic plastic deformation associated with some kind of structural changes induced by nanoindentation. Previous studies of other semiconductor materials have revealed a number of plastic deformation mechanisms occurring as a result of mechanical loading by using nanoindentation and cross-

sectional transmission electron microscopy (XTEM) techniques, including densification by micro-cracking [16] and slip by punching out of dislocation arrays [11,25–27]. Furthermore, the reverse discontinuities during unloading curve, the so-called "pop-out" event commonly observed in silicon and has been attributed to pressure-induced phase transition [28,29], is not observed here. Therefore, it is clear that the pop-in event may reflect the transition from perfectly elastic to plastic deformation, that is, it is the onset of plasticity in GaN:Mg thin film. The corresponding shear stress under the Berkovich indenter at indentation load P_{cr}, where the load-displacement discontinuity occurs, can be determined by using the following relation [30]:

$$\tau_{\max} = 0.31\left(\frac{6P_{cr}E_{film}^2}{\pi^3R^2}\right)^{1/3} \quad (7)$$

where R is the tip radius of the indenter. Comparisons of the mechanical properties of the present GaN:Mg thin films with those reported by previous studies are also presented in Table 1. It can be seen that Mg-doping does have the enhancement effects on various mechanical properties of the GaN:Mg films, presumably due to the solute hardening effects arisen from the size difference between Ga and Mg atoms.

Finally, in order to check if there is any influence from the substrate in a more quantitative manner, especially when the studying objects are thin films, it is essential to monitor the mechanical properties as a function of depth. For the present case, it is noted that the events of multiple pop-ins are coinciding nicely with sudden decreases in the hardness of measured materials [31]. As can be seen in Fig. 4(b), the hardness of GaN:Mg thin film decreases abruptly at the penetration depth of ~30 nm corresponding to the pop-in event. The hardness after the pop-in for GaN:Mg thin film remains nearly constant with small fluctuations, possibly associated with dislocation activities. Similarly, as shown in Fig. 4(c), the Young's modulus of GaN:Mg thin films also displays a sudden drop occurring around the same penetration depth and then remains relatively constant. Consequently, it is plausible to state that indentation with contact depths being less than 30% of the total film thickness is needed to obtain intrinsic thin film properties and minimize the influence from the substrate [32].

4. Conclusion

To summarize, the structural features, electrical and mechanical characteristics of GaN:Mg thin films obtained by using MOCVD process with the various Cp2Mg flow rates are investigated by XRD, AFM, Hall measurement and nanoindentation techniques. The XRD and AFM results suggest that overdoped films resulting from high Cp2Mg flow rates may have led to degradations in film crystalline structure by introducing excessive dislocation density, which in turn not only dramatically alters the film surface morphology and surface roughness but also reduces the effective hole concentrations. The Hall measurements evidently indicate that the highest hole concentration of 3.1×10^{17} cm^{-3} is achieved for films obtained with the Cp2Mg flow rate of 25 sccm. Nanoindentation results indicated that both the Young's modulus and film hardness are increased with increasing Mg doping concentration. The typical values obtained for the former ranges from 20.5 ± 0.9 to 28.5 ± 1.6 GPa and that for the latter ranges from 308.2 ± 2.6 to 409.8 ± 6.6 GPa for GaN:Mg thin films deposited with various Cp2Mg flow rates of 25–100 sccm.

Acknowledgements

This work was partially supported by the National Science Council of Taiwan, under Grant Nos.: NSC98-2112-M155-001-MY3, NSC100-2221-E-214-024 and NSC101-2221-E-214-017. JYJ is partially supported by the NSC of Taiwan and the MOE-ATU program operated at NCTU. Author likes to thank Dr. Y.-S. Lai and Dr. P.-F. Yang for their technical supports.

References

[1] P. Kozodoy, H. Xing, S.P. DenBaars, U.K. Mishra, A. Saxler, R. Perrin, S. Elhamri, W.C. Mitchel, J. Appl. Phys. 87 (2000) 1832.
[2] C. Bayram, J.L. Pau, R. McClintock, M. Razeghi, Appl. Phys. Lett. 92 (2008) 241103.
[3] G. Kipshidze, V. Kuryatkov, B. Borisov, Y. Kudryavtsev, R. Asomoza, S. Nikishin, H. Temkin, Appl. Phys. Lett. 80 (2002) 2910.
[4] K.S. Kim, M.S. Han, G.M. Yang, C.J. Youn, H.J. Lee, H.K. Cho, J.Y. Lee, Appl. Phys. Lett. 77 (2000) 1123.
[5] X. Zhang, S.J. Chua, P. Li, K.B. Chong, W. Wang, Appl. Phys. Lett. 73 (1998) 1772.
[6] E.L. Waldron, J.W. Graff, E.F. Schubert, Appl. Phys. Lett. 79 (2001) 2737.
[7] G. Coli, K.K. Bajaj, J. Li, J.Y. Lin, H.X. Jiang, Appl. Phys. Lett. 78 (2001) 1829.
[8] J. Li, K.B. Nam, J.Y. Lin, H.X. Jiang, Appl. Phys. Lett. 79 (2001) 3245.
[9] L. Liu, G. Cao, X. Chen, J. Nanomater. 2008 (2008) 271763.
[10] T.H. sung, J.C. Huang, J.H. Hsu, S.R. Jian, Appl. Phys. Lett. 97 (2010) 171904.
[11] R. Navamathavan, Y.-T. Moon, G.S. Kim, T.G. Lee, J.H. Hahn, S.J. Park, Mater. Chem. Phys. 99 (2006) 410.
[12] S.R. Jian, Jason S.C. Jang, Y.S. Lai, P.F. Yang, C.S. Yang, H.C. Wen, C.H. Tsai, Mater. Chem. Phys. 109 (2008) 360.
[13] S.R. Jian, G.J. Chen, T.C. Lin, Nanoscale Res. Lett. 5 (2010) 935.
[14] S.R. Jian, W.C. Ke, J.Y. Juang, Nanosci. Nanotechnol. Lett. 4 (2012) 598.
[15] S.R. Jian, H.G. Chen, G.J. Chen, Jason S.C. Jang, J.Y. Juang, Curr. Appl. Phys. 12 (2012) 849.
[16] S.J. Bull, J. Phys. D. Appl. Phys. 38 (2005) R393.
[17] X.D. Li, B. Bhushan, Mater. Charact. 48 (2002) 11.
[18] W.C. Oliver, G.M. Pharr, J. Mater. Res. 7 (1992) 1564.
[19] R.R. Lieten, V. Motsnyi, L. Zhang, K. Cheng, M. Leys, S. Degroote, G. Buchowicz, O. Dubon, G. Borghs, J. Phys. D: Appl. Phys. 44 (2011) 135406.
[20] S. Hautakangas, J. Oila, M. Alatalo, K. Saarinen, L. Liszkay, D. Seghier, H.P. Gislason, Phys. Rev. Lett. 90 (2003) 137402.
[21] A.F. Wright, U. Grossner, Appl. Phys. Lett. 73 (1998) 2751.
[22] J.C. Zhang, D.S. Jiang, Q. Sun, J.F. Wang, Y.T. Wang, J.P. Liu, J. Chen, R.Q. Jin, J.J. Zhu, H. Yang, T. Dai, Q.J. Jia, Appl. Phys. Lett. 87 (2005) 071908.
[23] P. Vennéguès, M. Benaissa, B. Beaumont, E. Feltin, P. De Mierry, S. Dalmasso, M. Leroux, P. Gibart, Appl. Phys. Lett. 77 (2000) 880.
[24] I. Waki, F. Fujioka, M. Oshima, H. Miki, A. Fukizawa, Appl. Phys. Lett. 78 (2001) 2899.
[25] C.H. Tsai, S.R. Jian, J.Y. Juang, Appl. Surf. Sci. 254 (2008) 1997.
[26] J.E. Bradby, J.S. Williams, J. Wong-Leung, M.V. Swain, P. Munroe, Appl. Phys. Lett. 78 (2001) 3235.
[27] J.E. Bradby, S.O. Kucheyev, J.S. Williams, J. Wong-Leung, M.V. Swain, P. Munroe, G. Li, M.R. Phillips, Appl. Phys. Lett. 80 (2002) 383.
[28] S.R. Jian, Nanoscale Res. Lett. 3 (2008) 6.
[29] S.R. Jian, G.J. Chen, J.Y. Juang, Curr. Opin. Solid State Mater. Sci. 14 (2010) 69.
[30] K.L. Johnson, Contact Mechanics, Cambridge University Press, Cambridge, UK, 1985.
[31] J.E. Bradby, J.S. Williams, M.V. Swain, J. Mater. Res. 19 (2004) 380.
[32] X.D. Li, H.S. Gao, C.J. Murphy, L.F. Gou, Nano Lett. 10 (2004) 1903.